

Investigation of optical and dispersion parameters poly vinyl alcohol doped Safranin O dye (PVA/SO) thin film

F. Bahrani*, I. K. Jasim, A. Q. Abdullah

Department of Physics, College of Science, Basrah University, Basrah – Iraq

Optical characteristics of polyvinyl alcohol/Safranin O dye (PVA/SO) thin films prepared by casting technique have been examined. Compositions and crystalline features of PVA/SO thin films are investigated with X-Ray Diffraction analyses. Ultraviolet–Visible spectroscopy has been utilized to measure the absorption and transmission optical properties of the thin films through the wavelength range 300-900 nm. Two regions can be recognized in absorption coefficient related to the direct band gaps, which are about 3.93 eV of the fundamental energy gap and 2.11 eV of the onset gap. The theoretical Wemple-DiDomenico model has been performed to quantify the static refractive index n and the dispersion energy in addition to the oscillation energy (E_o). The results reveal that the data of the refractive index dispersion in this model obeyed the single oscillator, which is used to deduce the dispersion and the high frequency dielectric constant. In the examined wavelength range, it has been investigated the complex dielectric constant of PVA/SO dye thin films. The ratio of the carrier concentration to the effective mass has been estimated. Oscillation energy values have been examined in this study by describing the expression $E_o \approx E_g$ and checking the Wemple-DiDomenico model. PVA/SO thin films have interesting physical properties for solar cell applications.

(Received December 18, 2023; Accepted February 19, 2024)

Keywords: Optical properties, Polyvinyl alcohol, Refractive index, Safranin O dye, Wemple-DiDomenico single oscillator model

1. Introduction

Polymers and dyes combination, amongst functional macromolecules, have a great potential research field with respect to high performance materials. Based on that, colored polymers in recent years have become significantly substantial for many technical applications and a fundamental part of lifestyle. Nowadays, diverse applications of dye-containing polymers are used in painting industries, medicine, gas separation processes [1], DSSC [2], nonlinear optics (NLO) [3], light emitting diode (LED) [4], and optical storage devices [5]. Due to the stability and optical bleaching of these organic materials, their applications are usually limited in devices. Therefore, more stable dye is required to design new potential hybrid systems, such as encapsulated dye molecules in gel host. Clearly these applications are associated with the dye's nature that combines with the identical polymer; the specific polymers affinity is invested in wastewater work ups. Dyes are colored due to the selective absorption of light in the visible spectrum region (400-700 nm), possess at least one chromophore, and have a conjugated system, such as molecules structure with single and double alternating bonds (C-C and C=C bonds) which prepare the material with the π -electron delocalization, However, it is also linked to the intensity of light, as well as exhibit electrons resonance [6]. The color can be lost if any of these features in the molecular structure are missing. Besides chromophores, auxochromes groups (color helpers) also exist in many dyes, such as hydroxyl groups, amino, sulfonic acid and carboxylic acid. Whilst their existence is not responsible for the color, they do color shifting and are usually utilized to affect the solubility of the dye. Many researches have embedded it to include dyes within polymers to obtain thin films that enable us to take advantage of the good properties of polymers, such as mechanical properties and resistance to organic solvents and temperatures. A suitable host material, PVA, is used among the diverse polymers since it has outstanding features, such as water solubility, chemical stability, perfect film forming character, charge storage

* Corresponding authors: fatimah.hameed@uobasrah.edu.iq
<https://doi.org/10.15251/JOBM.2024.161.35>

capacity, easy process ability, as well as dielectric strength, high transmittance and flexibility [7]. Actually, the organic compound is widely utilized in the optoelectronics applications technology, such as biological applications, textile industries, tannin mordant and silk, and dye wool. Basic dyes are among the various dyes currently available and are one of the brightest classes of soluble dyes that are employed in textile industries. Basic dye is called a cationic dye and it is a positive charge (cationic) that could interact with a negatively charged (anionic) material. Moreover, 3,7-Diamino-2,8-dimethyl-5-phenylphenazin-5-ium chloride represents the IUPAC name for the Safranin (O) dye. An organic dye typical example is Safranin (O) which is known as Basic Red 2 and belongs to Quinone-Imine class.

Besides the enormous applications of Safranin (O) in dye industries, it is as well utilized as a biological staining, which is well known to be toxic to human and animals, in a number of biomedical research laboratories [8][9]. Absorption spectroscopy indicates to a mechanism which measures the electromagnetic radiation absorption as a wavelength or frequency. According to the absorption process that occurs as a result of the interaction between the sample and electromagnetism, this could be explained by the differences in the absorption spectra. An absorption spectrum is polymer material or molecule fingerprint. To study interactions between radiation and electrons, UV-Vis absorption has been utilized as a common analytical tool. However, infrared absorptions are usually utilized to analysis the interaction between the electromagnetic waves and the energy of the vibration of the bonds [10]. Whilst optical constants are expected to prepare more physical information concerning the spectral dependence of optical parameters, such as extinction coefficient, absorption coefficient, refractive index and real and imaginary dielectric constant, which are important in characterizing the materials employed in the optoelectronic devices fabrication [11].

The aim of this research is to evaluate the optical characteristic of PVA/SO dye thin film and to illustrate the refractive index dispersion in terms of the Wemple-DiDomenico WDD model, a single oscillator model.

2. Experimental

Thin films have been provided from the prepared dye using the casting method, due to the ease of this method, and the possibility of preparing thin films of different thicknesses by dissolving 0.5g of PVA provided by Aldrich in 5ml of dimethyl formaldehyde ($\text{H.CO.N(CH}_3)_2(\text{DMF})$) provided from Thomas Baker as a solvent, and shaking the mixture by means of a mechanical mixer at room temperature for about an hour. Then the safranin dye ($\text{C}_{20}\text{H}_{19}\text{ClN}_4$), provided by BDH chemical Ltd., was added to the solution, by dissolving 0.025g of the dye into solution. Then the mixture was shaken well until a homogeneous solution was obtained, after which it was kept in a dry place and then poured. The solution was placed on a glass substrate that had been carefully cleaned by immersing it in a cleaning solution consisting of acetone and exposing it to a stream of distilled water. After drying, the glass substrates were placed on a horizontal level and some drops added on the glass substrate and left until dry for at least 24 hr. to ensure the solvent volatilizes, after which it was thermally treated at a temperature of 50°C. UV-Vis spectroscopy type Shimadzu-1800 at the range 200-1100 nm was used to measure the spectral absorbance.

3. Results and discussion

The crystalline structure of the PVA/SO dye thin film has been performed using an XRD diagnostic on the thin film sample, see Fig. 1. It is clear that in the X-ray diagram there is one broad diffraction peak only of the PVA/SO compound showing that it originates from PVA, which agrees with the reported literature [12]. The (101) peak of the crystalline thin film has been obtained at 19.90° ($d=4.46^\circ\text{\AA}$) and corresponds to a monoclinic unit cell [13], and superimposed on a broad hump ($14^\circ\text{--}30^\circ$) reflecting the amorphous content of the compound. Safranin O hydrated

structure resulting from the interaction between Safranin O dye and PVA can be eliminated by hydrogen bonding [14]. Equation 1 is used to calculate the particle size. X-ray line broadening analysis has been used to estimate the average grain size of the samples by Scherer's formula [15]:

$$D = \frac{k\lambda}{\beta \cos \theta} \quad (1)$$

where K is Scherer's factor, usually taken as 0.94. λ is the X-ray wavelength, β is the FWHM value in degree unit and transform to radian by multiplying $(\pi/180)$ and θ is the Bragg angle where $D=15.32$ nm for PVA/SO dye thin film. Ghoshal et al. found the grain size of PVA/BTB dye about $17.74\text{--}18.58^\circ\text{A}$ at different concentration of dyes. The crystal size is used to estimate the number of defects and vacancies in the crystal, which is known as the dislocation density and can be calculated by [16]:

$$\delta = 1/D^2 \quad (2)$$

where δ represents the dislocation density, the δ value is about $4.26 \times 10^{-3} \text{m}^{-2}$, and D is the size of the average crystallite.

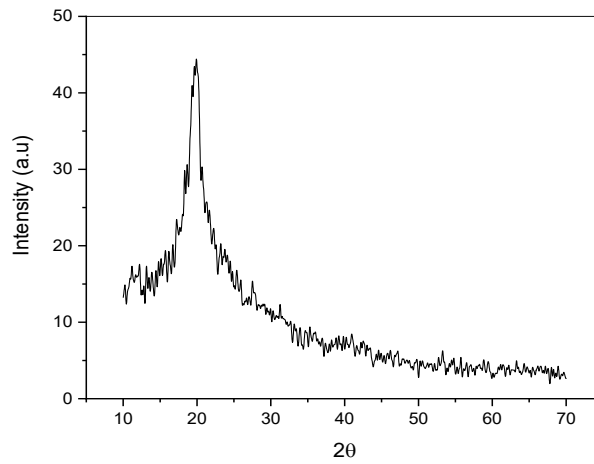


Fig. 1. XRD of PVA/SO dye thin film.

The optical properties of PVA/SO dye composite thin film is calculated by using UV–Vis spectroscopy in the range of 300–900 nm, as illustrated in Fig. 2 and Fig. 3, respectively. The absorbance peaks are increasing with increase of the wavelength with the maximum peaks at the range 400–600 nm. The prepared sample cleared absorbance peaks at nearly 525 nm. Fig. 3 shows the transmittance spectrum increase at the large wavelength where the sample appears as transparent. Fig. 4 indicates the reflectance spectrum for the sample according to equation [17]

$$A+T+R=1 \quad (3)$$

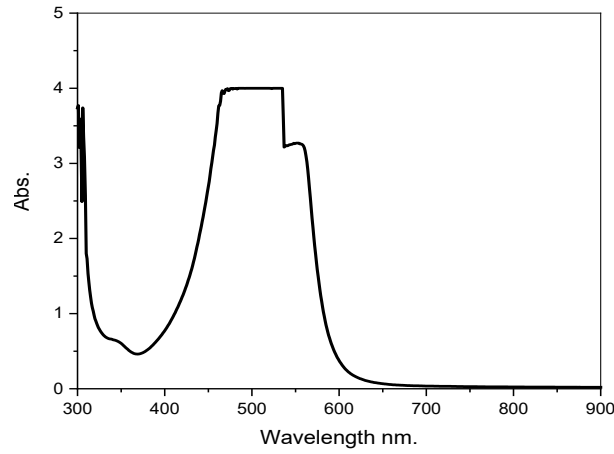


Fig. 2. The absorption spectral for PVA/SO film

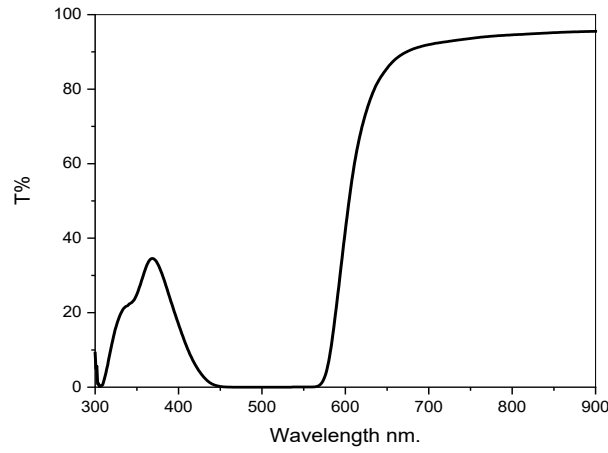


Fig. 3. The transmission spectral for PVA/SO film.

From Fig. 4, high reflecting characteristics beyond around 600 nm reach 70% and then decrease in the large wavelength owing to the increased probability of photons lacking the necessary energy to interact with electrons or atoms reflecting [18]. Fig. 5 show the α as a function of the incident photon [19]:

$$\alpha = \frac{2.303}{d} A \quad (4)$$

We noticed that α increased rapidly with increased photon incident. α analysis as a function of the photon energy ($h\nu$) near the fundamental absorption edge with exciton effects neglected and has been used to calculate the optical energy band-gap (E_g) and the optical transition type for crystalline and non-crystalline thin film by the expression [20][21]:

$$(\alpha h\nu)^m = B (h\nu - E_g) \quad (5)$$

where B is a constant, h represents the Plank's constant, ν is the light frequency and m is the material transition nature ($m = 2$ or $\frac{1}{2}$ for direct and indirect transition, respectively).

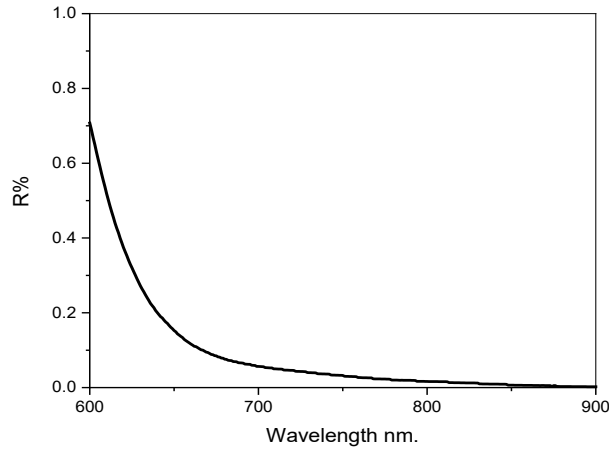


Fig. 4. Reflectance spectral as a function of wavelength for PVA/SO film

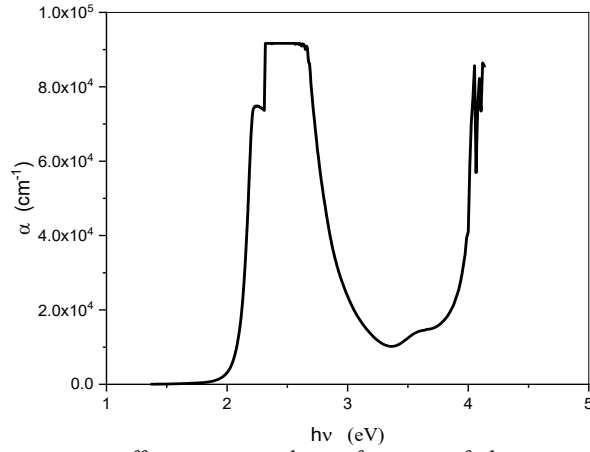


Fig. 5. The absorption coefficient spectral as a function of photon energy for PVA/SO film.

The E_g of PVA/SO dye thin film is calculated by plotting the relation between $(\alpha h\nu)^2$ as a function of $h\nu$ as illustrated in Fig. 6. Two significant regions can be recognized related to energy gaps; the values of the fundamental energy gap (E_{gf}) and onset gap (E_{go}) were determined to be 3.93eV and 2.11 eV, respectively. This behavior is clear in many previous studies, where the polymer absorbs in the UV region, while the dye absorption is within the visible region. It is also noted that there is a clear displacement of the energy gap of PVA near short photon energy [16].

The E_g with filling tends to decrease. This may be attributed to the fact that small amounts of incorporation of doping can form charge transfer complexes in the host matrix. Accordingly, the electrical conductivity increases due to the charge transfer complexes by providing additional charge, thus reducing the energy gap [22].

In general, the tail width in the E_g of localized defect states represents the Urbach energy. Indeed, this disorder is related with structural defects in the thin film, which lead to an elongation of the state's density in the band tails. Defects are produced by impurities which enhance the intermediate levels in the E_g . The width of the exponential absorption edge is taken into consideration in the Urbach energy E_u , and can be calculated by [23].

$$\alpha = \alpha_0 \exp\left(\frac{h\nu}{E_u}\right) \quad (6)$$

where α_0 represents a constant. The plots of PVA/SO dye in Fig. 7 shows $\ln(\alpha)$ as a function of $h\nu$. The linear fit slope ($1/E_u$) of the $\ln(\alpha)$ versus $(h\nu)$ plots gives the E_u values, as shown in Fig. 7. Thus, E_u values are around 143.6meV.

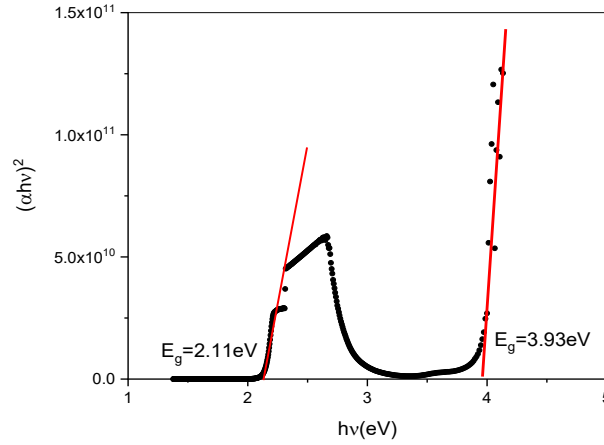


Fig. 6. Plot of $(\alpha h\nu)^2$ vs. $h\nu$ for PVA/SO film.

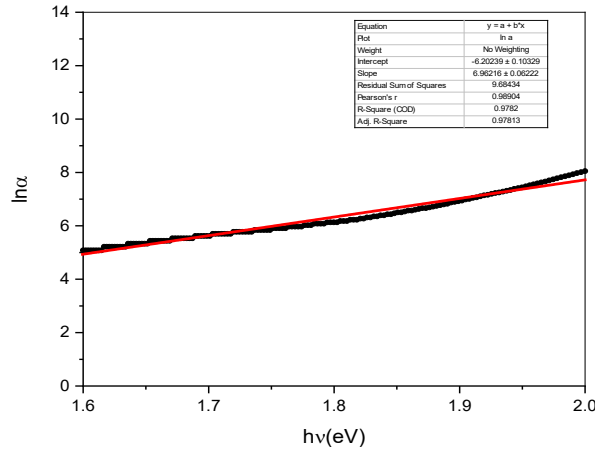


Fig. 7. Plot of $\ln \alpha$ vs. $h\nu$ for PVA/SO film.

The extinction coefficient (k) has been associated with the α according to the following relationship [24].

$$k = \alpha \lambda / 4\pi \quad (7)$$

For PVA/ SO film, Fig. 8 shows the relation between k and wavelength (λ). As seen, high value of k is caused by the increase in the atomic refractions number as a result of the enhancement in the linear polarizability [25]. The value of the refraction index (n) provides the thin film optical characteristics and is given by the equation [26].

$$n = \left(\frac{1 + \sqrt{R}}{1 - \sqrt{R}} \right) \quad (8)$$

n variation as a function of wavelength, see Fig. 9. The studied samples have shown that n reduces sharply when wavelength is enhanced from 600 nm to 700 nm; then in the high photon energy region it becomes saturated. The refractive index dispersion relies on the light beam frequency. The $h\nu$ dependence on n has been investigated utilizing the single effective oscillator model of WDD model [27] as:

$$n^2 = 1 + \frac{E_o E_d}{E_o^2 - (h\nu)^2} \quad (9)$$

where E_d and E_o represent single oscillator constants. E_d is the energy of the dispersion, which is regarded as a direct measure of the optical transitions' average strength between the bands. E_o is the energy of the single oscillator, which is regarded as the average excitation energy of the electronic transition; it is related to the E_g .

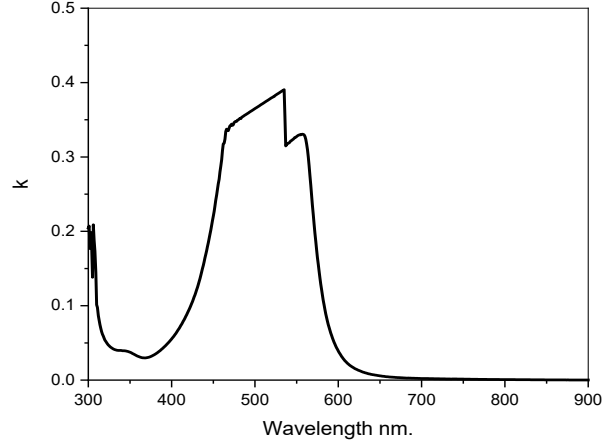


Fig. 8. The extinction coefficient as a function of wavelength for PVA/SO film

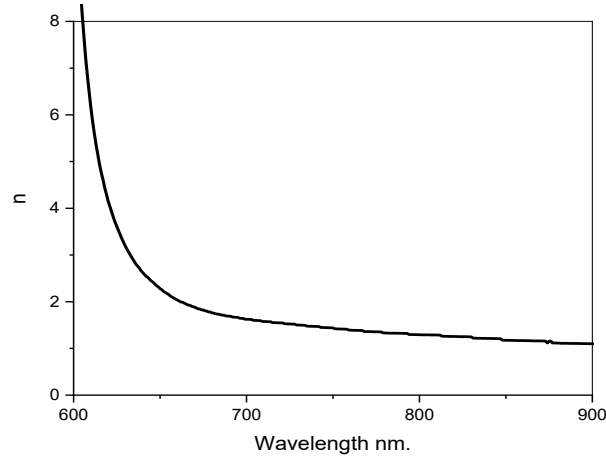


Fig. 9. The values of refractive index as a function of wavelength for PVA/SO film.

The $(n^2 - 1)^{-1}$ and $(h\nu)^2$ curves are plotted in Fig. 10; the linear part of the curve reaches close to the band edge, where this linear fit is valid near the optical energy gap to straight line with slope $(-1/E_o E_d)$ and the intersection $(E_o E_d)$. The calculated dispersion parameters of E_d and E_o are shown in Table 1. The E_o value is changed in the same way with the energy gap, while E_d is based on the distribution of the charge within a unit cell, which is closely associated with chemical bonding. Dispersion has an important role in terms of optical communication and spectral dispersion.

Table 1. PVA/SO thin film optical constants.

Quantity	Value	Quantity	Value
$E_o (eV)$	2.98	$\lambda_o (nm)$	425
$E_d (eV)$	4.08	$S_o (m^{-2})$	1.08×10^{13}
$M_{-1} (eV)^2$	1.96	$N / m^* (m^3.kg)^{-1}$	1.22×10^{40}
$M_{-3} (eV)^2$	0.45	ε_∞	13.66

The static refractive index value (n_o) has been estimated by extrapolating the WDD model dispersion equation to ($h\nu \rightarrow 0$), which is obtained by [28]:

$$\varepsilon_r(0) = \lim_{h\nu \rightarrow 0} (n^2(h\nu)) = n_o^2 = 1 + \frac{E_d}{E_o} \quad (10)$$

The calculated value of n_o is about 1.72. The high frequency dielectric constant, $\varepsilon_o = (n_o)^2$, is 2.96. E_o and E_d according to the WDD model are associated to the imaginary part ε_2 of the complex dielectric function, and the optical spectrum moments (-1 and -3) of the ε_2 has been derived from the expression below [29]:

$$E_o^2 = \frac{M_{-1}}{M_{-3}}, \quad E_d^2 = \frac{M_{-1}^3}{M_{-3}} \quad (11)$$

The M_{-1} and M_{-3} moments values are summarized in Table 1, where M_{-1} is dimensionless and M_{-3} is in eV. The complex dielectric function (ε^*) in terms of its real and imaginary is often expressed by the equation [30]:

$$\varepsilon^* = \varepsilon_1 + \varepsilon_2 = (n^*)^2 = (n + ik)^2 \quad (12)$$

The real (ε_1) and imaginary (ε_2) parts of the dielectric permittivity have been evaluated utilizing the complex refractive index, as given:

$$\varepsilon_1 = n^2 - k^2, \varepsilon_2 = 2nk \quad (13)$$

The real part of dielectric constant ε_1 is related to the square of wavelength λ^2 by the following formula [31].

$$\varepsilon_1 = n^2 - k^2 = \varepsilon_\infty - B\lambda^2 \quad (14)$$

$$B = \frac{e^2}{4\pi^2 c^2 \varepsilon_o} \frac{N}{m^*} \quad (15)$$

ε_∞ is infinite high frequency dielectric constant, e is the electronic charge, ε_o is the free space permittivity (8.854×10^{-12} F/m), c is the light velocity, and the ratio of the carrier concentration to the effective mass is N/m^* . Fig. 11 shows the relation between n^2 as a function of λ^2 . The linear part of this dependence is extrapolated to zero wavelength to give ε_∞ value, and from the slope the N/m^* values can be estimated according to the Eq. 15. ε_∞ and N/m^* values are listed in Table 1. The oscillator model is also given as [32]

$$n^2 - 1 = S_o \lambda_o^2 \left[1 - \left(\frac{\lambda_o}{\lambda} \right)^2 \right] \quad (16)$$

where λ represents the incident radiation wavelength, λ_o is as average oscillator wavelength, and S_o is as average oscillator strength.

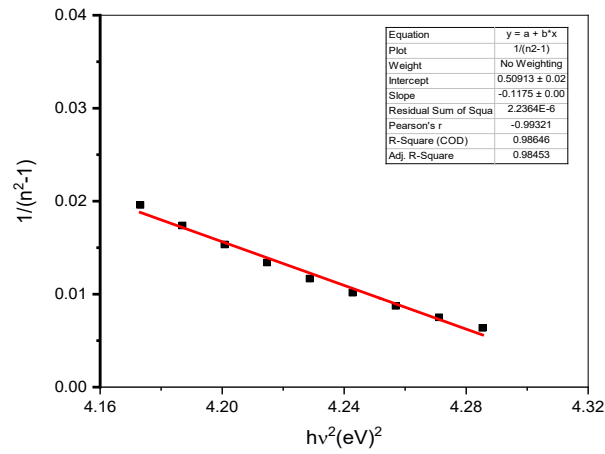


Fig. 10. $(n^2-1)^{-1}$ as a function of $h\nu^2$ for PVA/SO film.

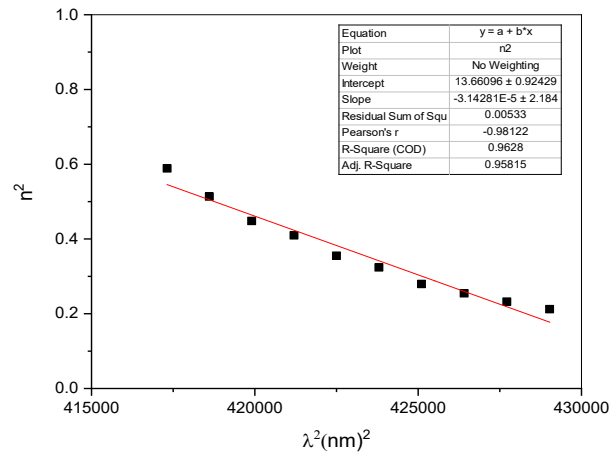


Fig. 11. n^2 as a function of λ^2 for PVA/SO film.

The plots of $(n^2 - 1)^{-1}$ as a function of the λ^{-2} as shown in Fig. 12 have been fitted into straight lines according to the formula of Meier's dispersion. The intersection between the slope $(1/S_0)$ and the infinity wavelength $(1/S_0 \lambda_0)^2$ gives the estimated value of S_0 and λ_0 . The values of the optical parameters are listed in Table 1.

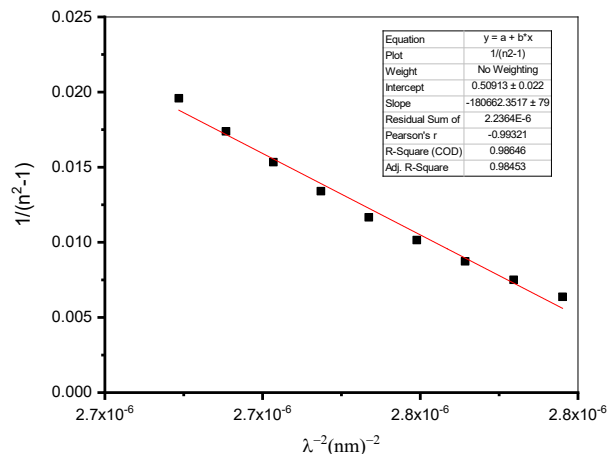


Fig. 12. The plotting $(n_o^2-1)^{-1}$ verses λ^{-2} for PVA/SO film.

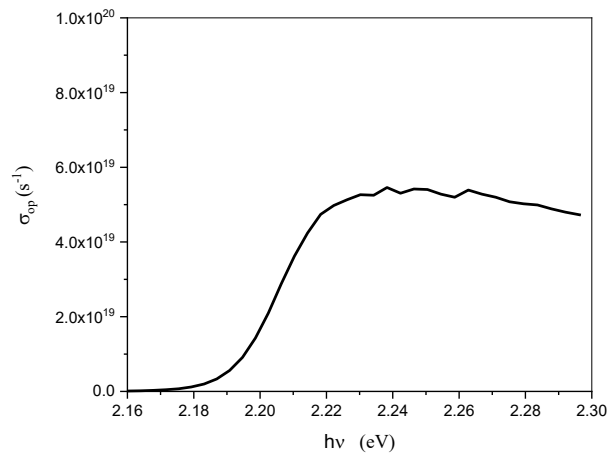


Fig. 13. The optical conductivity as a function of $h\nu$ for PVA/SO film.

Optical conductivity (σ_{op}) is one of the significant quantities which is fundamentally utilized to detect any further allowed inter-band optical transition of the material, and describe the solids optical properties [33]:

$$\sigma_{op} = \frac{\alpha n c}{4\pi} \quad (17)$$

The σ_{op} versus the $h\nu$ is shown in Fig. 13, and it is obvious that σ_{op} increases as $h\nu$ increases.

4. Conclusions

PVA/SO dye thin film was deposited using cast method technique. The optical and structural properties of the PVA/SO dye have been investigated. XRD analyses revealed that the thin film is semi-crystalline. Optical study of the thin films shows that direct energy gaps are low at 3.93eV and 2.11eV, respectively, and E_u is about 143.6 meV. The thin film optical behavior has been described well using the WDD model. The spectral dependence of optical parameters, such as extinction coefficient, refractive index linear and nonlinear optical susceptibilities, real and imaginary parts of the complex optical conductivity, the complex impedance, the complex electric modulus, and dielectric function, in the photon energy range (1.54-4.9 eV) have been performed using UV-Vis spectrophotometer experiments. The deduced values for the high frequency dielectric, single oscillator energy and static refractive index were derived from the linear portion of the $(n^2-1)^{-1}$ versus $(h\nu)^2$ plots utilizing the WDD model. Energy gap values satisfy this expression $E_o \approx 1.4E_g$.

References

- [1] C. Fleischmann, M. Lievenbrück, H. Ritter, Polym. 7(4), 717 (2015); <https://doi.org/10.3390/polym7040717>
- [2] D. Devadiga et al., Surfaces and Interfaces 33 102236 (2022); <https://doi.org/10.1016/j.surfin.2022.102236>
- [3] A. Y. Al-Ahmad, G. M. Shabeeb, A. Q. Abdullah, K. M. Ziadan, Optik (Stuttg). 122 (21), 1885 (2011); <https://doi.org/10.1016/j.ijleo.2010.11.018>
- [4] Ali Q. Abdullah, Salah Sh. Al-Luaibi, Karema M. Zaidan, basrah J. Sci (A). 27 (1) 52 (2009).
- [5] A. Natansohn, P. Rochon, M. S. Ho, C. Barrett, Macromolecules 28 (12), 4179 (1995);

<https://doi.org/10.1021/ma00116a019>

- [6] E. N Abrahart, Dyes and their intermediates, Edward Arnold Amazon Books (1977).
- [7] K. Deshmukh et al., Polym. Plast. Technol. Eng. 55(3), 231 (2016),
- [8] Soyab Salim Bagwan, photocatalytic degradation of hazardous Safranin (O) dye by using self synthesized TiO₂ nanoparticles
- [9] R. A. Almotiri, M. M. Alkhamisi, A. R. Wassel, A. M. El-Mahalawy, Mater. Res. Bull. 151, 111824 (2022); <https://doi.org/10.1016/j.materresbull.2022.111824>
- [10] A. N. Alias, Z. M. Zabidi, A.M.M. Ali, M. K. Harun, M.Z.A. Yahya, International Journal of Applied Science and Technology 3(5), (2013).
- [11] T. S. (Trevor S. Moss, G. J. Burrell, B. Ellis, Semiconductor opto-electronics, p. 441 (1973).
- [12] G. H. Chen, F. Y. Wang, C. F. Mao, and C. H. Yang, J. Appl. Polym. Sci., vol. 105 (3), 1086 (2007); <https://doi.org/10.1002/app.26257>
- [13] S. Gupta et al., Colloids Surf. B. Biointerfaces, 74(1), 186(2009); <https://doi.org/10.1016/j.colsurfb.2009.07.015>
- [14] H. M. P. Naveen Kumar et al., Carbohydr. Polym., vol. 82(2), 251 (2010); <https://doi.org/10.1016/j.carbpol.2010.04.021>
- [15] M. J. Chithra, M. Sathya, K. Pushpanathan, Acta Metall. Sin. (English Lett., vol. 28 (3), 394(2015); <https://doi.org/10.1007/s40195-015-0218-8>
- [16] D. Ghoshal, D. Bhattacharya, D. Mondal, S. Das, N. Bose, M. Basu, J. Polym. Res., 28(3), (2021); <https://doi.org/10.1007/s10965-021-02452-x>
- [17] A. H. A. Darwesh et al., Coatings 13(3), 578 (2023); <https://doi.org/10.3390/coatings13030578>
- [18] A. A. Alshehri, M. A. Malik, J. Mater. Sci. Mater. Electron. 30(17), 16156 (2019); <https://doi.org/10.1007/s10854-019-01985-8>
- [19] M. M. Kareem et al., J. Garmian Univ., 4(4), 1 (2017); <https://doi.org/10.24271/garmian.217>
- [20] E. A. Davis, N. F. Mott, Philos. Mag. 22(179), 903 (1970); <https://doi.org/10.1080/14786437008221061>
- [21] Tauc, J., Ed., The optical properties of solids, New York : Academic Press, (1966).
- [22] C. U. Devi, A. K. Sharma, V. V. R. N. Rao, Mater. Lett. 56 (3), 167 (2002); [https://doi.org/10.1016/S0167-577X\(02\)00434-2](https://doi.org/10.1016/S0167-577X(02)00434-2)
- [23] F. Urbach, Phys. Rev.92(5), 1324 (1953); <https://doi.org/10.1103/PhysRev.92.1324>
- [24] Ali Qassim Abdullah, Alaa Yassin Al-Ahmad, Hadi Ziara Al-Sawaad, Walailak J Sci & Tech 10(2), 159(2013).
- [25] Ali Qassim Abdullah, Salah Sh. El-Lauibi, Eman M. Jaboori, Int. J. Nanoelectronics and Materials 7, 65 (2014).
- [26] Ahmed Saud Abed, Kreema M. Ziadan and Ali Qassim Abdullah, Iraqi J. of Polymers 17 (1), 18 (2014).
- [27] S. H. Wemple, M. DiDomenico, Phys. Rev. B 3(4), 1338 (1971); <https://doi.org/10.1103/PhysRevB.3.1338>
- [28] A. El Hachmi, B. Manoun, Int. J. Mater. Res.114(2), 100 (2023); <https://doi.org/10.1515/ijmr-2022-0189>
- [29] Z. Z. You, G. J. Hua, J. Alloys Compd. 530, 11 (2012); <https://doi.org/10.1016/j.jallcom.2012.03.078>
- [30] Fox M., Optical properties of solids, Oxford University Press: New York, (2001)
- [31] T.S Moss, G.J. Burrell, B. Ellis, Semiconductor Opto-Electronics, Butterworth-Heinemann, (2013).
- [32] Anusha Mony, Sheelakumari Issac, Jayakumari Isac, International Journal of Science and Research (IJSR), 3(12), (2014).
- [33] I. M. El Radaf, Appl. Phys. A 126(5), (2020); <https://doi.org/10.1007/s00339-020-03543-0>